



University of Groningen

## Thermal Gradient Mid- and Far-Infrared Spectroscopy as Tools for Characterization of Protein Carbohydrate Lyophilizates

Mensink, M. A.; Šibík, J.; Frijlink, H. W.; Maarschalk, K. van der Voort; Hinrichs, W. L. J.; Zeitler, J. A.

*Published in:*  
Molecular pharmaceutics

*DOI:*  
[10.1021/acs.molpharmaceut.7b00568](https://doi.org/10.1021/acs.molpharmaceut.7b00568)

**IMPORTANT NOTE:** You are advised to consult the publisher's version (publisher's PDF) if you wish to cite from it. Please check the document version below.

*Document Version*  
Publisher's PDF, also known as Version of record

*Publication date:*  
2017

[Link to publication in University of Groningen/UMCG research database](#)

### *Citation for published version (APA):*

Mensink, M. A., Šibík, J., Frijlink, H. W., Maarschalk, K. V. D. V., Hinrichs, W. L. J., & Zeitler, J. A. (2017). Thermal Gradient Mid- and Far-Infrared Spectroscopy as Tools for Characterization of Protein Carbohydrate Lyophilizates. *Molecular pharmaceutics*, 14(10), 3550-3557.  
<https://doi.org/10.1021/acs.molpharmaceut.7b00568>

### **Copyright**

Other than for strictly personal use, it is not permitted to download or to forward/distribute the text or part of it without the consent of the author(s) and/or copyright holder(s), unless the work is under an open content license (like Creative Commons).

### **Take-down policy**

If you believe that this document breaches copyright please contact us providing details, and we will remove access to the work immediately and investigate your claim.

*Downloaded from the University of Groningen/UMCG research database (Pure): <http://www.rug.nl/research/portal>. For technical reasons the number of authors shown on this cover page is limited to 10 maximum.*

# Thermal Gradient Mid- and Far-Infrared Spectroscopy as Tools for Characterization of Protein Carbohydrate Lyophilizates

M. A. Mensink,<sup>†,‡,§,||</sup> J. Šibík,<sup>§,||,⊥</sup> H. W. Frijlink,<sup>†</sup> K. van der Voort Maarschalk,<sup>†,#</sup> W. L. J. Hinrichs,<sup>\*,†</sup> and J. A. Zeitler<sup>\*,||</sup>

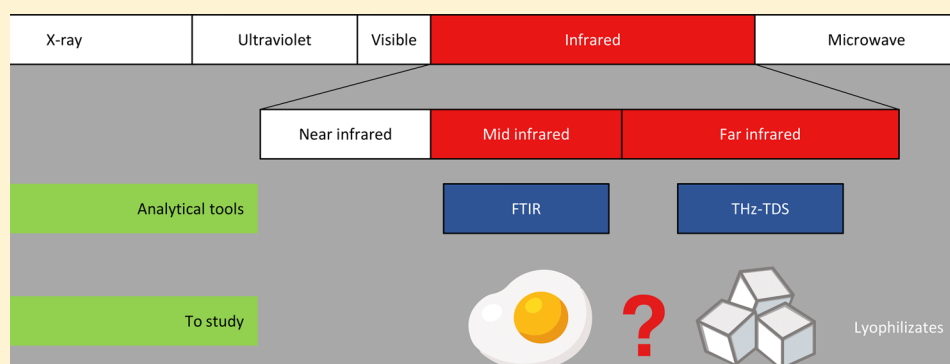
<sup>†</sup>Department of Pharmaceutical Technology and Biopharmacy, University of Groningen, Antonius Deusinglaan 1, 9713 AV Groningen, The Netherlands

<sup>‡</sup>Janssen Vaccines and Prevention, Archimedesweg 4, 2333 CN Leiden, The Netherlands

<sup>§</sup>Department of Chemical Engineering and Biotechnology, University of Cambridge, Philippa Fawcett Drive, Cambridge CB3 0AS, United Kingdom

<sup>⊥</sup>F. Hoffmann-La Roche A.G., Basel 4070, Switzerland

<sup>#</sup>Process Technology, Corbion Purac, P.O. Box 21, 4200 AA Gorinchem, The Netherlands



**ABSTRACT:** Protein drugs play an important role in modern day medicine. Typically, these proteins are formulated as liquids requiring cold chain processing. To circumvent the cold chain and achieve better storage stability, these proteins can be dried in the presence of carbohydrates. We demonstrate that thermal gradient mid- and far-infrared spectroscopy (FTIR and THz-TDS, respectively) can provide useful information about solid-state protein carbohydrate formulations regarding mobility and intermolecular interactions. A model protein (BSA) was lyophilized in the presence of three carbohydrates with different size and protein stabilizing capacity. A gradual increase in mobility was observed with increasing temperature in formulations containing protein and/or larger carbohydrates (oligo- or polysaccharides), lacking a clear onset of fast mobility as was observed for smaller molecules. Furthermore, both techniques are able to identify the glass transition temperatures ( $T_g$ ) of the samples. FTIR provides additional information as it can independently monitor changes in protein and carbohydrate bands at the  $T_g$ . Lastly, THz-TDS confirms previous findings that protein–carbohydrate interactions decrease with increasing molecular weight of the carbohydrate, which results in decreased protein stabilization.

**KEYWORDS:** terahertz time-domain spectroscopy (THz-TDS), Fourier transform infrared spectroscopy (FTIR), hydrogen bonding, molecular mobility, solid state

## 1. INTRODUCTION

Over the past decades, the proportion of biopharmaceuticals among new drugs has gradually increased. In 2014, seven of the 10 best-selling drugs were proteins.<sup>1</sup> These proteins are typically formulated as solutions, which require cold chain processing. Cold storage and transportation are both costly and impractical, particularly in developing countries. To overcome the need for refrigeration, proteins can be dried in the presence of one or more stabilizing excipients to produce a more thermally stable formulation. Drying is mostly done by either spray- or freeze-drying, and carbohydrates are frequently used as stabilizers during processing. Carbohydrates need to meet

certain criteria to be good stabilizers:<sup>2</sup> first, carbohydrates need to be able to replace water during drying by replacing the hydrogen bonds between water and the protein;<sup>3,4</sup> second, the carbohydrate should form an amorphous matrix that exhibits a high enough glass transition temperature,  $T_g$ , such that the molecular mobility of the protein is strongly reduced. Characterization of protein–carbohydrate interactions and

**Received:** July 5, 2017

**Revised:** August 23, 2017

**Accepted:** September 5, 2017

**Published:** September 5, 2017

molecular mobility of protein carbohydrate lyophilizates in the solid state can therefore aid in protein formulation development. Here we discuss which information can be obtained for this purpose using Fourier transform infrared spectroscopy (FTIR) and terahertz time-domain spectroscopy (THz-TDS).

FTIR spectroscopy is frequently used for the determination of secondary structure of proteins and has also been used to show protein–carbohydrate interactions at ambient temperature.<sup>5–7</sup> Photons in the mid-infrared region can induce vibrational excitation of covalently bonded atoms and groups. The frequency at which these groups absorb radiation depends on the mass of the atoms involved and on the bonds affecting these groups (i.e., covalent bonds and hydrogen bonding).<sup>8</sup> A typical mid-infrared spectrum of a protein–carbohydrate mixture thus shows multiple bands originating from bending and stretching vibrations of specific chemical groups. Provided these bands do not overlap, this allows for simultaneous analysis of protein specific groups and carbohydrate specific groups. Monitoring the frequency of these peaks as a function of temperature can provide information on changes in interactions with that group (i.e., hydrogen bonding).<sup>9</sup> This can indirectly provide insight about the onset of mobility of specific groups as a function of temperature and about protein–carbohydrate interactions.

More recently it was demonstrated that THz-TDS can be used to study intermolecular interactions, such as changes in the strength of the hydrogen bonds between molecules in liquids and solids.<sup>10</sup> From a practical application point of view THz-TDS can be considered a far-IR extension of FTIR. In liquids and amorphous solids THz-TDS spectra fall into the spectral range where high-frequency dielectric relaxations overlap with the onset of the vibrational modes that are characteristic for the disordered structure, the so-called vibrational density of states (VDOS).<sup>11,12</sup> The VDOS is composed of phonon-like vibrations albeit without strong resonant character due to the lack of the periodic molecular network that is characteristic of crystalline solids. The VDOS thus exhibits a single broad spectral feature, that spans the majority of the frequency range accessible by typical THz-TDS instruments (0.2–4 THz). Yet, given the intermolecular nature of the VDOS, THz-TDS can be used as a sensitive probe of the molecular dynamics of amorphous samples both above and below  $T_g$ . We were previously able to show that terahertz spectroscopy is sensitive to both primary and secondary relaxations,<sup>13,14</sup> with the former reflecting global mobility and the latter local molecular mobility far below  $T_g$ . The mechanism of interaction between THz radiation and molecules is experimentally linked to the mean squared molecular displacement commonly measured by inelastic neutron scattering (INS),<sup>15–17</sup> and hence, THz-TDS is capable of providing similar insight into the protein dynamics<sup>18–21</sup> and may offer a more accessible benchtop alternative measurement technology to INS.<sup>22</sup>

Recently, it was shown that smaller and molecularly more flexible carbohydrates stabilize proteins better than larger and more rigid carbohydrates do, provided they maintain sufficient vitrification.<sup>23</sup> This was explained in terms of the fact that the smaller and more flexible carbohydrates are less affected by steric hindrance and therefore better suited to form hydrogen bonds with the protein.<sup>6</sup> In this work we examine freeze-dried protein–carbohydrate samples using carbohydrates of different sizes and molecular flexibility and evaluate the ability of FTIR and THz-TDS to measure protein–carbohydrate hydrogen

bonding and thermally induced changes in mobility in the amorphous state. In particular, a small disaccharide (trehalose), a molecularly flexible oligosaccharide (inulin), and a molecularly rigid polysaccharide (dextran) are used in combination with an elaborately studied protein (BSA). These carbohydrates were chosen as their protein stabilizing capacities were shown to be different due to their differences in size and molecular flexibility with four model proteins of varying characteristics.<sup>2,23</sup>

## 2. METHODS

**2.1. Materials.** Bovine serum albumin (BSA) was acquired from Sigma-Aldrich (Zwijndrecht, The Netherlands), trehalose was purchased from Cargill (Amsterdam, The Netherlands), dextran 70 kDa was obtained from Pharmacomos (Holbaek, Denmark), and inulin 1.8 kDa was a generous gift from Sensus (Roosendaal, The Netherlands).

**2.2. Freeze-Drying.** Each carbohydrate and BSA was dissolved in ultrapure water to a concentration of 100 mg/mL. 10 mL vials of type 6R (type I glass, Fiolax clear, Dedecke, Königswinter, Germany) were filled with 1 mL of a specific formulation. For the protein–carbohydrate mixtures 200  $\mu$ L of BSA solution and 800  $\mu$ L carbohydrate solution were used, achieving a 1:4 (w/w) protein–carbohydrate ratio. All samples were produced simultaneously, using the same stock BSA solution to reduce the risk of sample variability. The vials were placed on the precooled (278 K) shelf of a Christ Epsilon 2-4 freeze-dryer (Salm & Kipp, Breukelen, The Netherlands). Freezing was done by cooling the shelf to 233 K with intermediate isothermal periods of 30 min at 278 and 268 K. All cooling and heating was done at a rate of 1 K/min unless otherwise mentioned. The shelf was kept at 233 K for an hour, after which the pressure was lowered to 87  $\mu$ bar while the temperature was raised to 248 K. Primary drying was done under these conditions during 24 h. For secondary drying, the shelf temperature was increased to 313 K at 0.1 K/min, after which the temperature was maintained for 6 h. The vials were closed using rubber stoppers at 87  $\mu$ bar and additionally crimped with aluminum seals upon removal from the freeze-drier. Samples were stored at ambient temperature for 3 months followed by another 3 months of storage at 278 K. The samples were stored in closed vials, and the vacuum was maintained in the vials for all the samples up until the moment of analysis.

**2.3. Terahertz Time-Domain Spectroscopy.** Particular care was taken to minimize influence of atmospheric moisture on the results of the terahertz measurements, as the lyophilized samples are hygroscopic. Water exhibits very strong terahertz absorption, and the presence of water molecules is well-known to have a significant effect on the molecular mobility in the sample. The final sample preparation, from opening the vials to mounting the sample in the sample holder, took place in a glovebag (Sigma-Aldrich AtmosBag) purged with dry nitrogen gas (relative humidity <1%) to avoid moisture sorption from atmospheric water vapor. The lyophilized cake was broken up using a spatula, and the powder was pressed into a tablet of 13 mm diameter using a load of 2 metric tons. The resulting tablets were wedged between 2 z-cut quartz windows of 3 mm thickness each and placed in a copper sample holder. Another slot on the same copper sample holder was loaded with a set of two reference z-cut quartz windows. The sample holder was attached to a cryostat with a motorized linear translation stage that allowed switching between the sample and reference slots, and placed into a vacuum chamber of a home-built THz-TDS

setup, as described elsewhere.<sup>13</sup> The cryostat was first cooled to 80 K and then heated to either 460 or 500 K, depending on sample, with 20 K increments. The temperature was controlled using a LakeShore 331 temperature controller. We allowed 10 min for thermal equilibration at each temperature point. The THz-TDS setup allows measurement of absorption spectra and refractive index spectra between 0.3 and 3.0 THz. The terahertz data were analyzed following the procedure proposed by Duvillaret et al.<sup>24</sup> When reporting thermal change in terahertz absorption as a function of temperature, we use the frequency of 1 THz as it provides the best signal-to-noise ratio as outlined previously.<sup>14</sup>

**2.4. Attenuated Total Reflectance Fourier-Transform Infrared Spectroscopy (ATR-FTIR).** In addition to the THz-TDS measurements, FTIR spectra of the samples were collected using a Tensor 27 spectrometer (Bruker Optics, Etlingen, Germany) equipped with a high temperature Golden Gate Mark II attenuated total reflectance accessory (Specac Slough, United Kingdom). The complete spectrometer was placed in a glovebag (Sigma-Aldrich Atmosbag) and continually purged with nitrogen gas to eliminate atmospheric water. The vials containing the lyophilized powder were only opened inside the glovebag. A sample of few milligrams was placed on the diamond window without further sample preparation and pressed down in a controlled fashion using the torque-limited anvil. Samples were analyzed from 323 K up to a maximum temperature in the range of 423 to 533 K, depending on the carbohydrate in the mixture, at a continuous ramp rate of 1 K/min. The temperature accuracy of the heater was verified using five melting point standards ranging from 320–322 K to 506–511 K. Measurements were carried out every 2 min. Spectra were collected between 4000 and 850  $\text{cm}^{-1}$  at a resolution of 4  $\text{cm}^{-1}$ , and 64 scans were taken during approximately 1 min and averaged for each measurement. Spectra were collected for both pure carbohydrate samples and colyophilized protein–carbohydrate mixtures. Matlab software (Mathworks, Natick, MA, United States of America) was used to process the obtained FTIR spectra using a custom built script. In brief, the following actions were subsequently performed: ATR correction, atmospheric correction, spectral smoothing, background subtraction, and fitting of the FTIR peaks of interest to accurately determine frequency and intensity of the peak maxima. Bands of interest were the carbohydrate-specific band (950–1050  $\text{cm}^{-1}$ ), the protein specific amide I band (1600–1700  $\text{cm}^{-1}$ ), and the OH stretching vibration (vOH) band (3100–3600  $\text{cm}^{-1}$ ).

**2.5. Differential Scanning Calorimetry (DSC).** Previously reported differential scanning calorimetry (DSC) results of various carbohydrate formulations are used as reference for  $T_g$  values established by FTIR and THz-TDS.<sup>23</sup> For full practical details the reader is directed to the original manuscript. In brief, samples (about 2 to 3 mg) were analyzed in an open aluminum pan using a Q2000 DSC (TA Instruments, Ghent, Belgium). Samples were preheated for 3 min at 353 K to allow residual and/or adsorbed water to evaporate and subsequently cooled back to 293 K. Analysis was then done by heating the samples to 513 K at a rate of 20 K per minute. The inflection point of the step transition in the thermograph was taken as the  $T_g$ . The samples analyzed in that study contained negligible amounts of buffer (HEPES), whereas the samples in this study were lyophilized without buffer. This is not expected to have a relevant impact on the  $T_g$  values.

## 3. RESULTS

**3.1. Terahertz Spectroscopy.** **3.1.1. Frequency-Dependent Spectra.** The terahertz absorption spectra for pure BSA and pure carbohydrates are shown in Figure 1. Generally, the

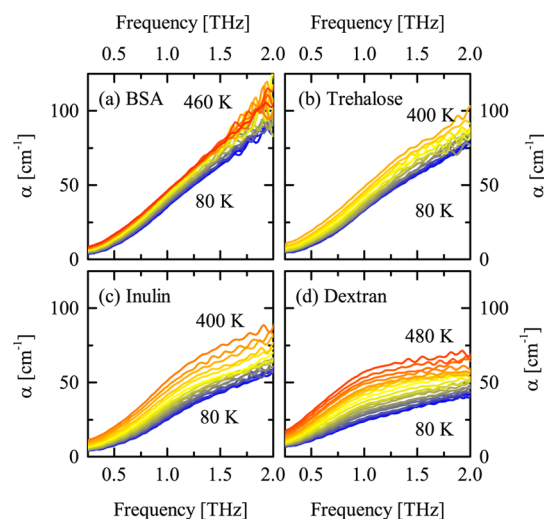


**Figure 1.** Terahertz absorption coefficient ( $\alpha$ ) of amorphous (a) BSA, (b) trehalose, (c) inulin 1.8 kDa, and (d) dextran 70 kDa over the temperature range 80–480 K. Data substantially above  $T_g$  are not shown as the amorphous tablets became structurally unstable and collapsed.

absorption increases with both temperature and frequency. The increase of absorption with frequency is expected, as it has been shown previously that the terahertz absorption is roughly proportional to the frequency squared up to the Ioffe–Regel limit (I–R limit),<sup>25,26</sup> above which phonon-like excitations become dispersed by disorder.<sup>12</sup> Qualitatively, the terahertz spectra suggest that the larger the molecule the lower the I–R limit. This would be expected intuitively, as in fully disordered systems any crossover between global and local disorder shifts to larger length scales, and hence can be observed at lower wavelengths. In addition, the intramolecular motions are expected to couple to the intermolecular motions, hence resulting in a stronger scattering of phonon-like intermolecular excitations. The most pronounced example is the case of dextran, where it may be concluded that the I–R limit is below 1.0 THz, given the strong flattening of the absorption above 1.0 THz. Surprisingly, BSA (66 kDa) does not show such a shoulder despite having a molecular mass similar to that of dextran (70 kDa). We presume that these differences originate from the differences in molecular structure between this carbohydrate and protein.

**3.1.2. Temperature-Dependent Spectra.** The temperature-induced changes in the terahertz absorption coefficient and refractive index at 1.0 THz are shown in Figure 2. Given that in all cases the same protein was used, the data for BSA in panels a–f is identical and is plotted repeatedly for clarity. The results are discussed further combined with interpretation in Discussion.

**3.2. ATR-FTIR.** Changes in the protein (amide I band, 1600–1700  $\text{cm}^{-1}$ ), carbohydrate (carbohydrate band, 950–1050  $\text{cm}^{-1}$ ), and overall sample (OH band, 3100–3600  $\text{cm}^{-1}$ ) as a function of temperature as established by ATR-FTIR are shown in Figure 3. The results are discussed further combined with interpretation in Discussion.



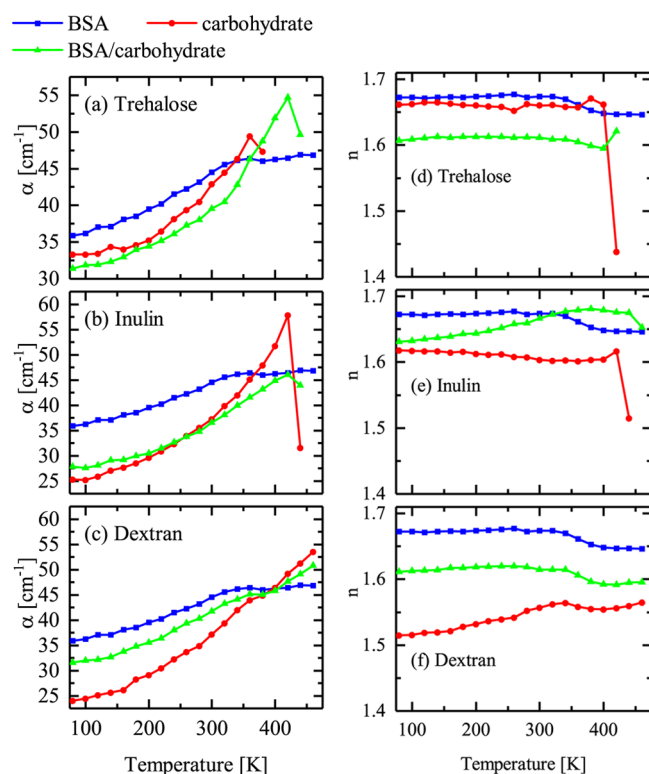


**Figure 2.** Left: Absorption coefficient ( $\alpha$ ) at 1.0 THz for (a) trehalose, (b) inulin 1.8 kDa, and (c) dextran 70 kDa, together with the absorption spectra of BSA and a 1:4 mixture of BSA and respective carbohydrate as a function of temperature. Right: Refractive index ( $n$ ) at 1 THz for (d) trehalose, (e) inulin 1.8 kDa, and (f) dextran 70 kDa, together with that of BSA and a 1:4 mixture of BSA and respective carbohydrate as a function of temperature.

## 4. DISCUSSION

**4.1. Effect of Molecular Size on Temperature Dependence of Terahertz Absorption.** In general, the terahertz absorption coefficient of all formulations is observed to increase with temperature. Such behavior is expected as the molecular mobility in disordered systems is enhanced when temperature increases. This is valid at temperatures both above and below the  $T_g$ , albeit for different reasons. Below the  $T_g$  the increase in terahertz absorption is linked to what is often referred to as the local mobility originating from Johari–Goldstein relaxation and its effect on the caged dynamics.<sup>27</sup> More recently we were able to show that the Johari–Goldstein process can be best understood from a physical point of view in terms of the potential energy surface (PES) model originally proposed by Goldstein where the intra- and intermolecular interactions of the molecules in the amorphous solid are confined by time- and temperature-dependent barriers.<sup>28</sup> The molecular configurations at low temperatures, below  $T_g$  in the Johari–Goldstein relaxation regime, are restricted to the local energy minima in the PES, and hence dynamics are significantly restricted. Above  $T_g$  the absorption increases strongly with temperature due to the onset of the primary relaxation which is possible once sufficient thermal energy is available to overcome the local potential wells allowing for local mobility as well as large scale conformational changes that are required for the primary relaxation dynamics.<sup>27</sup> In our measurements this increase in mobility was sufficient for the sample tablets of freeze-dried

materials to collapse, and thus we do not show any data above  $T_g$  as the measurement becomes unreliable.

For most samples absorption was observed to increase gradually from 80 K upon heating, but in the case of pure trehalose a pronounced increase in absorption is only evident at temperatures above 200 K (Figure 2). This behavior is likely linked to the different molecular sizes of the formulations. Compared to inulin and dextran, trehalose is a relatively small carbohydrate as it is a disaccharide. In such a system the potential energy barriers are relatively fewer in number than in the large and more flexible systems such as BSA, inulin, and dextran. Hence, larger scale conformational changes are needed to transition from one basin to another. As a consequence the Johari–Goldstein relaxation takes place only at higher temperatures for the small disaccharide, similarly to what was observed in small polyalcohols.<sup>14,27</sup> The larger molecules have more accessible states which become activated gradually upon heating, resulting in a more gradual increase in THz absorption. From Figure 2 one may notice that the larger the molecule is, the more gradual the increase in THz absorption is with temperature. For trehalose the increase below 200 K is only marginal while above 200 K it is relatively rapid. For dextran, inulin, and BSA the increase is parabolic from 80 K onward, becoming closer to linear with a larger molecular size.

For pure BSA the increase in terahertz absorption ceases from around 340 K onward upon heating. Similarly, we observe a drop in refractive index of BSA between 320 and 400 K (see Figure 2). This behavior cannot be ascribed to any changes in protein structure, as confirmed by the absence of any event below 470 K in the FTIR results (see Figure 3). Instead, we speculate that these changes originate from the evaporation of residual moisture (i.e., moisture not removed during lyophilization) from the protein sample. When a tablet prepared from an amorphous substance contains some moisture, it can escape from the sample during the THz-TDS measurement when performed in vacuum, as has been shown previously for amorphous polyvinylpyrrolidone/vinyl acetate.<sup>29</sup> Freeze-dried BSA can be expected to contain 2–4% w/w residual moisture after freeze-drying.<sup>23</sup> Secondary drying was conducted at 313 K at 87  $\mu\text{bar}$ ; it is possible that heating well above this temperature in vacuum during the THz-TDS measurement would result in the evaporation of this last, tightly bound water.

**4.2. Glass Transition.** Both THz-TDS and ATR-FTIR spectroscopies are very sensitive to the changes in molecular dynamics associated with the glass transition. Generally, terahertz absorption is expected to increase significantly when the molecules regain their mobility corresponding to the primary dielectric relaxation, allowing an easy determination of  $T_g$ .<sup>13,14</sup> In our case the opposite is observed in Figure 2. The reason for this is the sample format. While the previous studies considered homogeneous nonporous amorphous sample, the lyophilized cakes that were analyzed in this study were pressed into porous tablets. Upon heating beyond  $T_g$  the sample softens, becomes mechanically unstable, and collapses. This effectively lowers the beam path for the terahertz radiation and appears as a drop in the absorption coefficient. Hence, rather than deducting  $T_g$  from the molecular response, in this case one can determine it from the bulk sample response.

Due to the nature of the ATR measurement, the spectra are strongly influenced by the mechanical contact between the sample and the ATR crystal. Hence, the overall picture can only be obtained by combining the temperature effects on intramolecular vibrations and bulk thermal effects. From IR

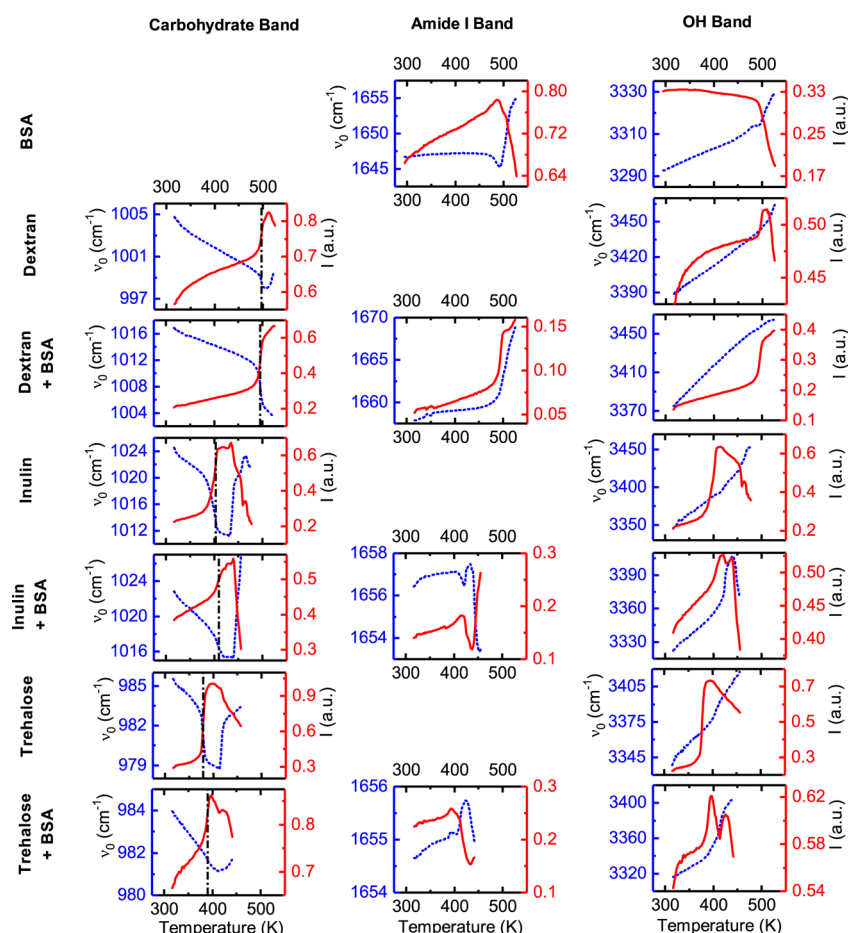


**Figure 3.** Frequencies ( $\nu_0$ ) and absorption intensities ( $I$ ) of the carbohydrate band (950–1050  $\text{cm}^{-1}$ ), amide I band (1600–1700  $\text{cm}^{-1}$ ), and OH-stretch band (3100–3600  $\text{cm}^{-1}$ ) of various lyophilized amorphous carbohydrates (trehalose, inulin 1.8 kDa, and dextran 70 kDa) with and without BSA from 323 K up to above their  $T_g$  (various temperatures). Dot-dashed vertical line in carbohydrate band column marks the  $T_g$  (see Table 1).

spectroscopy theory, one would expect lower and broader IR peaks upon heating the sample as the higher temperature would result in a broader spread of the population across the vibrational states. The increasing signal intensity in the ATR-FTIR seen in Figure 3 is thus not a result of a stronger molecular absorption, but in the absence of chemical changes in the sample it indicates an improved contact between the sample and the ATR diamond. Around the  $T_g$  of the sample, the sample softens due to an increase in global molecular mobility. Due to the gravity and the anvil pressing down on the sample, the softer sample results in a better sample contact and therewith increased signal intensity. It is thus possible to detect the glass transition by monitoring the change in intensity over temperature.

Table 1 shows the comparison in  $T_g$  as measured by THz-TDS (drop in absorption coefficient), FTIR (inflection point of change in carbohydrate band intensity), and DSC for the different carbohydrates. The THz-TDS and DSC measurements match well considering the relatively low resolution of 20 K used in the THz-TDS measurements. The  $T_g$  for dextran could not be clearly deduced from the THz-TDS results as it occurs in the proximity of the maximum temperature reachable by the used cryostat.

The ATR-FTIR estimates significantly lower  $T_g$  than DSC for trehalose and inulin. There can be in principle three possible reasons for this. First, the heating rate for DSC was 20 K/min, while the heating rate for FTIR was only 1 K/min. It is

**Table 1. Comparison of Glass Transition Temperature as Established by Traditional Method (DSC) and the Results Obtained Here Using ATR-FTIR and THz-TDS**

	THz-TDS	ATR-FTIR	DSC <sup>23</sup>
effect	steep change in absorption coefficient	inflection point of change in carbohydrate band intensity	inflection point of change in heat capacity
resolution (temp between measurements)	20 K	2 K	n/a
	$T_g$ (K)		
trehalose	380	379	395 ± 1
inulin 1.8 kDa	420	403	413 ± 2
dextran 70 kDa	n/a	497	496 ± 1
trehalose + BSA	440 <sup>a</sup>	390	n/a
inulin 1.8 kDa + BSA	440 <sup>a</sup>	410	n/a
dextran 70 kDa + BSA	n/a	495	n/a

<sup>a</sup>The changes in absorption coefficient were less abrupt and at higher temperatures for the protein–carbohydrate mixtures, presumably because BSA reduced the onset of viscous flow.

known that the detected glass transition temperature can be somewhat higher at faster heating rates, due to thermal lag/time needed for the relaxations to occur.<sup>30</sup> However, one would expect a similar effect on THz-TDS results, as the applied heating rate was similar to that of FTIR, which is not observed.

Another explanation for such a difference could be that the physical aging and relaxation of the amorphous system shifts the mechanical softening of the glass to the sub- $T_g$  region, as can be observed by thermomechanical analysis.<sup>31</sup> However, the samples used for the THz-TDS, FTIR, and DSC measurements were all aged similarly, excluding this explanation. We therefore conclude that the most likely reason for the lower ATR-FTIR glass transition is the plasticizing role of residual moisture. While the majority of water is removed during freeze-drying, about 2–4% w/w of residual moisture can be expected in the samples.<sup>23</sup> For the DSC measurement, a preheating step at 353 K (80 °C) was applied for several minutes before the measurement, to remove remaining water. For FTIR and THz-TDS measurement no such preheating step has been applied. Even such a small amount of water is known to strongly plasticize the samples and may reduce the  $T_g$  by 20 K or more, in line with the observation in the FTIR results in comparison to the DSC. The role of water is further supported by the results for dextran. It was previously reported that dextran is less hygroscopic than carbohydrates with a lower molecular weight.<sup>32</sup> This explains why the  $T_g$  observed by ATR-FTIR and DSC measurements matches well for dextran but not for trehalose and inulin.

Note that a temperature step of 20 K was used for the terahertz method, which is much coarser and limits the resolution of the results. Also, THz-TDS measurements were performed under vacuum and residual moisture could escape the sample during heating, similar to the case of pure BSA.

**4.3. Protein–Carbohydrate Bonding.** **4.3.1. Terahertz Spectroscopy.** From the THz-TDS data we can extract qualitative information regarding the intermolecular protein–carbohydrate interactions, in a similar manner to the analysis of the molecular interaction in binary liquid mixtures.<sup>33</sup> When there is no interaction between the compounds in the mixture, the mixture is phase separated and the terahertz absorption of the mixture would be expected to be described by the linear combination of the terahertz response of the pure constituents. On the other hand, when the constituents form a rich intermolecular network, the system behaves as one unit, and it is expected that the overall terahertz absorption is lower than that of the constituents due to a disrupted original hydrogen-bonded network that exists in the pure constituents.<sup>34,35</sup>

For the smallest carbohydrate used here, trehalose, the absorption coefficients of the protein–carbohydrate mixture were lower than those of the individual constituent components (Figure 2, left side). This shows that there are strong interactions between trehalose and BSA. The effect is smaller for the larger molecule inulin, a flexible oligosaccharide. For the largest carbohydrate, the polysaccharide dextran (70 kDa), this reduction in absorption for the mixture is completely absent. The absorption coefficients of the mixture of dextran and BSA are precisely between those of the separate components at all temperatures, implying that the two components behave independently of one another as a physical mixture. Additionally, the dextran–BSA mixture shows a depression in absorption around 360 K similar to the behavior we observed for pure BSA. This further corroborates that the two molecular species have phase separated.

The results are in agreement with our previous findings, where we observed a decreasing protein–carbohydrate miscibility with increasing protein size.<sup>36</sup> In conclusion, the THz-TDS data confirm that smaller carbohydrates interact more with the protein than larger carbohydrates do. This is in

line with the hypothesis that smaller carbohydrates are less affected by steric hindrance, and it explains why they are more capable of maintaining protein functionality during storage.<sup>6,23</sup>

**4.3.2. ATR-FTIR.** The interaction between carbohydrate and protein can be understood by carefully comparing the behaviors of the carbohydrate, amide, and OH peaks in the IR spectra of the separate components with those of the mixtures. First, we can compare the changes of these peaks during the glass transition. When comparing the mixtures to the pure carbohydrates (Table 1), both trehalose and inulin show a slightly higher  $T_g$  and more gradual change in signal intensity over temperature during the glass transition. Such a difference is not observed in dextran with and without BSA. Most likely, this slower or more gradual glass transition is indicative of strong protein–carbohydrate interactions. Due to the fact that the protein has a much higher molecular weight and a more complex structure compared to trehalose and inulin, strong protein–carbohydrate interactions are likely to result in delayed mechanical effects of the glass transition, as observed here.

In addition we observe a strong decrease in frequency of the carbohydrate band in all formulations that accompanies the strong increase in signal intensity. A change in frequency is indicative of changed interactions with the group measured. It is intuitive that the number and strength of interactions between and with the carbohydrate hydroxyl groups change as the mobility increases. The amide I band of the protein embedded in trehalose and inulin shows a small change in frequency around the  $T_g$ , followed by a larger increase in frequency. A possible explanation is that at temperatures below the  $T_g$  the carbohydrate is maintaining the protein structure, but around the  $T_g$  the increased mobility leads to a loss of interaction between the protein and carbohydrate, in turn resulting in protein unfolding. Again, such phenomena are not found in the formulation with dextran and BSA. This too implies that trehalose and inulin tightly interact with BSA whereas BSA and dextran behave separately from one another, in line with previous findings.<sup>36</sup> Unfortunately the denaturation of BSA and the  $T_g$  of dextran occur at the same temperature, making it impossible to distinguish two separate events and confirm the presumed phase separation.

## 5. CONCLUSION

In summary, we show that temperature controlled THz-TDS and FTIR can provide useful information about solid-state protein carbohydrate formulations regarding mobility and intermolecular interactions. The increase in mobility in formulations containing protein and/or larger carbohydrates (oligo- or polysaccharides) was gradual with temperature, lacking a clear onset of fast mobility as is observed for smaller molecules. Furthermore, with both techniques the  $T_g$  of such samples can be observed. FTIR provides additional information as it can independently monitor changes in protein and carbohydrate bands during the  $T_g$ . Lastly, THz-TDS confirms previous findings that smaller carbohydrates (disaccharides) have more interactions with proteins compared to larger carbohydrates (oligo- or polysaccharides).

## AUTHOR INFORMATION

### Corresponding Authors

\*Antonius Deusinglaan 1, 9713 AV Groningen, The Netherlands. Tel: +31 50 363 2398. Fax: +31 50 363 2500. E-mail: W.L.J.Hinrichs@rug.nl.



\*Department of Chemical Engineering and Biotechnology, University of Cambridge, West Cambridge Site, Philippa Fawcett Drive, Cambridge CB3 0AS, United Kingdom. Tel: +44 (0)1223 334783. E-mail: [jaz22@cam.ac.uk](mailto:jaz22@cam.ac.uk).

#### ORCID

M. A. Mensink: [0000-0002-6961-7776](https://orcid.org/0000-0002-6961-7776)

J. A. Zeitler: [0000-0002-4958-0582](https://orcid.org/0000-0002-4958-0582)

#### Author Contributions

<sup>§</sup>M.A.M. and J.S. contributed equally.

#### Notes

The authors declare no competing financial interest.

### ACKNOWLEDGMENTS

This research was jointly financed by Royal FrieslandCampina, the European Union, European Regional Development Fund and The Ministry of Economic Affairs, Agriculture and Innovation, Peaks in the Delta, the Municipality of Groningen, the Provinces of Groningen, Fryslân, and Drenthe, and the Dutch Carbohydrate Competence Center. Furthermore, we acknowledge the support of the UK Engineering and Physical Sciences Research Council [EP/J007803/1].

### REFERENCES

- (1) King, S. The best selling drugs in 2014. [www.firstwordpharma.com/node/1263906](http://www.firstwordpharma.com/node/1263906) (accessed Jun 19, 2015).
- (2) Mensink, M. A.; Frijlink, H. W.; van der Voort Maarschalk, K.; Hinrichs, W. L. J. How Sugars Protect Proteins in the Solid State and during Drying (Review): Mechanisms of Stabilization in Relation to Stress Conditions. *Eur. J. Pharm. Biopharm.* **2017**, *114*, 288–295.
- (3) Chang, L. L. L.; Pikal, M. J. M. Mechanisms of Protein Stabilization in the Solid State. *J. Pharm. Sci.* **2009**, *98* (9), 2886–2908.
- (4) Grasmeijer, N.; Stankovic, M.; de Waard, H.; Frijlink, H. W.; Hinrichs, W. L. J. Unraveling Protein Stabilization Mechanisms: Vittrification and Water Replacement in a Glass Transition Temperature Controlled System. *Biochim. Biophys. Acta, Proteins Proteomics* **2013**, *1834* (4), 763–769.
- (5) Souillac, P. O.; Middaugh, C. R.; Rytting, J. H. Investigation of Protein/carbohydrate Interactions in the Dried State. 2. Diffuse Reflectance FTIR Studies. *Int. J. Pharm.* **2002**, *235* (1–2), 207–218.
- (6) Mensink, M. A.; Van Bockstal, P.-J.; Pieters, S.; De Meyer, L.; Frijlink, H. W.; van der Voort Maarschalk, K.; Hinrichs, W. L. J.; De Beer, T. In-Line near Infrared Spectroscopy during Freeze-Drying as a Tool to Measure Efficiency of Hydrogen Bond Formation between Protein and Sugar, Predictive of Protein Storage Stability. *Int. J. Pharm.* **2015**, *496* (2), 792–800.
- (7) Taylor, L. S. Sugar-Polymer Hydrogen Bond Interactions in Lyophilized Amorphous Mixtures. *J. Pharm. Sci.* **1998**, *87* (12), 1615–1621.
- (8) Barth, A. Infrared Spectroscopy of Proteins. *Biochim. Biophys. Acta, Bioenerg.* **2007**, *1767* (9), 1073–1101.
- (9) Imamura, K.; Ohya, K. I.; Yokoyama, T.; Maruyama, Y.; Kazuhiro, N. Temperature Scanning FTIR Analysis of Secondary Structures of Proteins Embedded in Amorphous Sugar Matrix. *J. Pharm. Sci.* **2009**, *98* (9), 3088–3098.
- (10) Parrott, E. P. J.; Zeitler, J. A. Terahertz Time-Domain and Low-Frequency Raman Spectroscopy of Organic Materials. *Appl. Spectrosc.* **2015**, *69* (1), 1–25.
- (11) Møller, U.; Cooke, D. G.; Tanaka, K.; Jepsen, P. U. Terahertz Reflection Spectroscopy of Debye Relaxation in Polar Liquids [Invited]. *J. Opt. Soc. Am. B* **2009**, *26* (9), A113.
- (12) Taraskin, S. N.; Simdyankin, S. I.; Elliott, S. R.; Neilson, J. R.; Lo, T. Universal Features of Terahertz Absorption in Disordered Materials. *Phys. Rev. Lett.* **2006**, *97* (5), 55504.
- (13) Sibik, J.; Shalae, E. Y.; Axel Zeitler, J. Glassy Dynamics of Sorbitol Solutions at Terahertz Frequencies. *Phys. Chem. Chem. Phys.* **2013**, *15* (28), 11931.
- (14) Sibik, J.; Elliott, S. R.; Zeitler, J. A. Thermal Decoupling of Molecular-Relaxation Processes from the Vibrational Density of States at Terahertz Frequencies in Supercooled Hydrogen-Bonded Liquids. *J. Phys. Chem. Lett.* **2014**, *5* (11), 1968–1972.
- (15) Cicerone, M. T.; Douglas, J. F.  $\beta$ -Relaxation Governs Protein Stability in Sugar-Glass Matrices. *Soft Matter* **2012**, *8* (10), 2983.
- (16) Cicerone, M. T.; Zhong, Q.; Johnson, J.; Aamer, K. A.; Tyagi, M. Surrogate for Debye–Waller Factors from Dynamic Stokes Shifts. *J. Phys. Chem. Lett.* **2011**, *2* (12), 1464–1468.
- (17) Capaccioli, S.; Ngai, K. L.; Ancherbak, S.; Pacaroni, A. Evidence of Coexistence of Change of Caged Dynamics at T<sub>G</sub> and the Dynamic Transition at T<sub>D</sub> in Solvated Proteins. *J. Phys. Chem. B* **2012**, *116* (6), 1745–1757.
- (18) Markelz, A. G.; Knab, J. R.; Chen, J. Y.; He, Y. Protein Dynamical Transition in Terahertz Dielectric Response. *Chem. Phys. Lett.* **2007**, *442* (4–6), 413–417.
- (19) He, Y.; Ku, P. I.; Knab, J. R.; Chen, J. Y.; Markelz, A. G. Protein Dynamical Transition Does Not Require Protein Structure. *Phys. Rev. Lett.* **2008**, *101* (17), 178103.
- (20) Lipps, F.; Levy, S.; Markelz, A. G. Hydration and Temperature Interdependence of Protein Picosecond Dynamics. *Phys. Chem. Chem. Phys.* **2012**, *14* (18), 6375.
- (21) Falconer, R. J.; Markelz, A. G. Terahertz Spectroscopic Analysis of Peptides and Proteins. *J. Infrared, Millimeter, Terahertz Waves* **2012**, *33* (10), 973–988.
- (22) Sibik, J.; Zeitler, J. A. Study of Disordered Materials by Terahertz Spectroscopy. In *Disordered Pharmaceutical Materials*; Wiley-VCH Verlag GmbH & Co. KGaA: Weinheim, Germany, 2016; Vol. 96, pp 393–426.
- (23) Tonnies, W. F.; Mensink, M. A.; de Jager, A.; van der Voort Maarschalk, K.; Frijlink, H. W.; Hinrichs, W. L. J. Size and Molecular Flexibility of Sugars Determine the Storage Stability of Freeze-Dried Proteins. *Mol. Pharmaceutics* **2015**, *12* (3), 684–694.
- (24) Duvillaret, L.; Garet, F.; Coutaz, J.-L. A Reliable Method for Extraction of Material Parameters in Terahertz Time-Domain Spectroscopy. *IEEE J. Sel. Top. Quantum Electron.* **1996**, *2* (3), 739–746.
- (25) Loffe, A. F.; Regel, A. R. Non-crystalline, amorphous, and liquid electronic semiconductors. *Prog. Semicond.* **1960**, *4*, 237–291.
- (26) Mott, N.; Davis, E. *Electronic Processes in Non-Crystalline Materials*; Oxford University Press: Oxford, 1971.
- (27) Sibik, J.; Zeitler, J. A. Direct Measurement of Molecular Mobility and Crystallisation of Amorphous Pharmaceuticals Using Terahertz Spectroscopy. *Adv. Drug Delivery Rev.* **2016**, *100*, 147–157.
- (28) Ruggiero, M. T.; Krynski, M.; Kissi, O.; Sibik, J.; Markl, D.; Tan, N. Y.; Arslanov, D.; Zande, W. Van; Redlich, B.; Timothy, M.; Grohgan, H.; Lobmann, K.; Rades, T.; Elliott, R. The Significance of the Amorphous Potential Energy Landscape for Dictating Glassy Dynamics and Driving Solid-State Crystallisation. *ChemRxiv* **2017**, DOI: [10.26434/chemrxiv.5328235.v1](https://doi.org/10.26434/chemrxiv.5328235.v1).
- (29) Sibik, J.; Zeitler, J. A. Terahertz Response of Organic Amorphous Systems: Experimental Concerns and Perspectives. *Philos. Mag.* **2016**, *96* (7–9), 842–853.
- (30) Fukuoka, E.; Makita, M.; Nakamura, Y. Glassy State of Pharmaceuticals. V. Relaxation during Cooling and Heating of Glass by Differential Scanning Calorimetry. *Chem. Pharm. Bull.* **1991**, *39* (8), 2087–2090.
- (31) Fukuoka, E.; Makita, M.; Nakamura, Y. Glassy State of Pharmaceuticals. IV. Studies on Glassy Pharmaceuticals by Thermo-mechanical Analysis. *Chem. Pharm. Bull.* **1989**, *37* (10), 2782–2785.
- (32) Tong, H. H. Y.; Wong, S. Y. S.; Law, M. W. L.; Chu, K. K. W.; Chow, A. H. L. Anti-Hygroscopic Effect of Dextran in Herbal Formulations. *Int. J. Pharm.* **2008**, *363* (1–2), 99–105.
- (33) Li, R.; D’Agostino, C.; McGregor, J.; Mantle, M. D.; Zeitler, J. A.; Gladden, L. F. Mesoscopic Structuring and Dynamics of Alcohol/Water Solutions Probed by Terahertz Time-Domain Spectroscopy and Pulsed Field Gradient Nuclear Magnetic Resonance. *J. Phys. Chem. B* **2014**, *118* (34), 10156–10166.



- (34) Venables, D. S.; Schmuttenmaer, C. A. Spectroscopy and Dynamics of Mixtures of Water with Acetone, Acetonitrile, and Methanol. *J. Chem. Phys.* **2000**, *113* (24), 11222.
- (35) Li, R.; D'Agostino, C.; McGregor, J.; Mantle, M. D.; Zeitler, J. A.; Gladden, L. F. Mesoscopic Structuring and Dynamics of Alcohol/Water Solutions Probed by Terahertz Time-Domain Spectroscopy and Pulsed Field Gradient Nuclear Magnetic Resonance. *J. Phys. Chem. B* **2014**, *118* (34), 10156–10166.
- (36) Mensink, M. A.; Nethercott, M. J.; Hinrichs, W. L. J.; van der Voort Maarschalk, K.; Frijlink, H. W.; Munson, E. J.; Pikal, M. J. Influence of Miscibility of Protein-Sugar Lyophilizates on Their Storage Stability. *AAPS J.* **2016**, *18*, 1225–1232.